Implantable and degradable antioxidant poly(ε-caprolactone)-lignin nanofiber membrane for effective osteoarthritis treatment

Ruiming Liang [a, 1], Jinmin Zhao[a, b, 1], Bo Li [a, 1] , Peian Cai [a, b], Xian Jun Loh [c], Chuanhui Xu [d] , Peng Chen [e, *], Dan Kai [c, *], Li Zheng [a, *]

Author contributions

Jinmin Zhao, Li Zheng and Peng Chen designed the experiments and wrote the manuscript. Synthesis and characterization of PCL-lignin copolymers and nanofibers were performed by Dan Kai and Xian Jun Loh. Bo Li, Ruiming Liang, Peian Cai and Chuanhui Xu performed all cell experiments including immunofluorescence, intracellular ROS detection, flow cytometry, qRT-PCR analyses, in vivo experiments and data analysis.

[a] Guangxi Engineering Center in Biomedical Materials for Tissue and Organ Regeneration & Guangxi Collaborative Innovation Center for Biomedicine, Life Sciences Institute, Guangxi Medical University, Nanning, 530021, China

[b] Department of Bone and Joint Surgery & Guangxi Key Laboratory of Regenerative Medicine, The First Affiliated Hospital of Guangxi Medical University, Guangxi Medical University, Nanning, 530021, China

[c] Institute of Materials Research and Engineering (IMRE), A*STAR, 2 Fusionopolis Way, #08-03 Innovis, Singapore 138634

[d] Department of Rheumatology, Allergy and Immunology, Tan Tock Seng Hospital, Singapore 308433

[e] School of Chemical & Biomedical Engineering, Nanyang Technological University, 62 Nanyang Drive, Singapore 637459

[1] Ruiming Liang, Jinmin Zhao and Bo Li contributed equally to this work.

* Corresponding author.

* Corresponding author. School of Chemical & Biomedical Engineering, Nanyang Technological University, 62 Nanyang Drive, Singapore 637459

* Corresponding author. Institute of Materials Research and Engineering (IMRE), A*STAR, 2 Fusionopolis Way, #08-03 Innovis, Singapore 138634

* Corresponding author. Guangxi Engineering Center in Biomedical Materials for Tissue and Organ Regeneration & Guangxi Collaborative Innovation Center for Biomedicine, Life Sciences Institute, Guangxi Medical University, Nanning, 530021, China.

E-mail addresses: chenpeng@ntu.edu.sg (Peng Chen), kaid@imre.a-star.edu.sg (Dan Kai), zhengli224@163.com (Li Zheng).

Keywords: lignin, nanofiber, oxidative stress, autophagy, osteoarthritis, antioxidant

Abstract

Osteoarthritis (OA) is one of the most common musculoskeletal disorders worldwide. Oxidative stress initiated by excessive free radicals such as reactive oxygen species (ROS) is a leading cause of cartilage degradation and OA. However, conventional injection or oral intake of antioxidants usually cannot provide effective treatment due to rapid clearance and degradation or low bioavailability. Here, a new strategy is proposed based on nanofibers made of poly(ε-caprolactone) (PCL) and PCL-grafted lignin (PCL-*g*-lignin) copolymer. Lignin offers intrinsic antioxidant activity while PCL tailors the mechanical properties. Quantified by ^{31}P NMR, PCL-g-lignin copolymer contained 0.64 mmol/g of aliphatic OH groups and 0.43 mmol/g phenolic OH groups, respectively. Electrospun PCL-lignin nanofibers showed excellent antioxidant activity, which inhibited almost 97.50% of free radicals after 48 h. PCL-lignin nanofibers also exhibit low cytotoxicity and excellent anti-inflammatory effects as demonstrated using both H_2O_2-stimulated human chondrocytes and an OA rabbit model. PCL-lignin nanofibers inhibit ROS generation and activate antioxidant enzymes through autophagic mechanism. Arthroscopic implantation of nanofibrous membrane of PCL-lignin is effective to OA therapy because it is biocompatible, biodegradable and able to provide sustained antioxidant activity.

Introduction

Osteoarthritis (OA) is a musculoskeletal disorder that affects over 250 million people worldwide [1, 2]. It causes joint pain, inflammation, swelling, and motion loss.

Progressive cartilage degradation, accompanied by synovial inflammation and subchondral bone damage, is the hallmark of OA [3, 4]. Currently, effective treatments for OA are lacking. The over-generation of free radicals by injured chondrocytes has been considered as the main mechanism of cartilage cell loss and tissue damage [5]. It has been reported that the amount of lipid peroxidation products (such as malondialdehyde (MDA) and reactive oxygen species (ROS)) dramatically increase in the joints of OA patients [6-8]. An increase in ROS production leads to hyper-peroxidation, protein carbonylation and DNA damage which alter chondrocyte function [9, 10]. ROS could also cause a disruption in cell signaling pathways that are redox-regulated and stimulate pro-death cell signaling pathways to compromise chondrocyte integrity and disrupt cartilage homeostasis cartilage damage, which eventually result in loss of cartilage function.[6, 11, 12]. Antioxidants such as phenols (like Vitamin E), ubiquinones (vitamin Q), flavonoids (like curcumin, quercetin), thiols (like glutathione or thioredoxin) [13, 14] and anti-oxidant materials (such as xanthan gum and alginate[15], dopamine melanin[16], fullerene and fullerol[17]), which can neutralize free radicals and thus decrease oxidative stress, are usually injected to delay or limit cellular damage and cartilage matrix degradation in OA joints. Some antioxidants reduce oxidative factors such as ROS, MDA, superoxide dismutase (SOD), glutathione (GSH), and catalase (CAT) by increasing the formation of autophagic vesicles, upregulating expression of crucial factors against oxidative stress (like nuclear factor erythroid 2-related factor 2 - NRF2), and activating antioxidant enzymes[18-20]. However, it is challenging to effectively deliver antioxidants because they are rapidly

cleared away from synovial joints. Therefore, repeated injection or oral administration is required, and consequently side-effects often arise.

A functional antioxidative scaffold that can sustainably and locally suppress oxidative stress is desirable for OA therapy. Lignin is a type of polyphenolic biopolymers found in plants [21]. It is abundant, cheap, biodegradable and of good mechanical strength. More interestingly, it can act as an antioxidant because its phenolic hydroxyl groups have excellent abilities to scavenge free radicals[22, 23]. Multiple functional groups such like phenolic, hydroxyl, and methoxyl groups in lignin can terminate oxidative chain reactions by efficiently neutralizing free radicals[24]. But lignin is brittle and of low viscosity, thus can hardly be electrospun to make fibrous membrane[25]. Lignin can be conjugated with other polymers, such as polyethylene glycol (PEG), isopropyl acrylamide, polypropylene, cellulose, poly (lactic acid) (PLA), etc by the way of ring opening polymerization, radical polymerization, atom transfer radical polymerization.[22, 26, 27] These copolymers can be readily fabricated into hydrogels, nanoparticles, and fiberous membranes for biomedical applications, such as wound dressing , drug/gene delivery and tissue engineering[28-33]. Our previous studies have demonstrated that lignin-based copolymers preserved the antioxidant activity[34]. However, they have been rarely utilized as antioxidative biomaterials for OA therapy.

In this study, we fabricated a new antioxidant copolymer poly(ε-caprolactone)-grafted lignin(PCL-*g*-lignin) by solvent-free ring-opening polymerization, and used its the nanofiberous electrospun membrane to treat OA for the first time. PCL serves to

enhance the mechanical properties while lignin acts as the antioxidant. The therapeutic effect and the underlying mechanism are investigated in vitro on human chondrocytes and in an OA rabbit model (**Figure 1**). This study shall provide a novel strategy for arthroscopic intervention of OA therapy based on the demonstrated implantable and biodegradable scaffolds with intrinsic and sustained antioxidant activities.

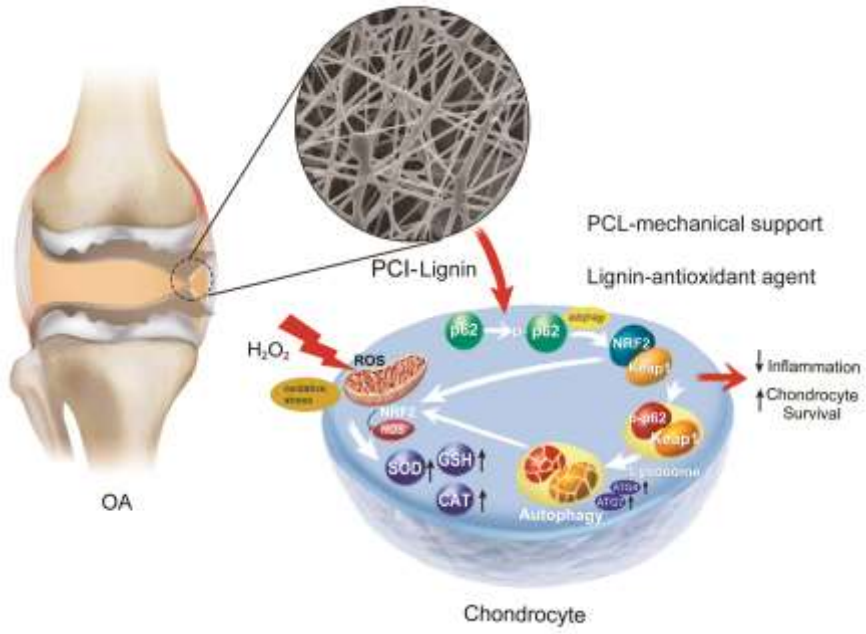

Figure 1. Schematic illustration of PCL-lignin nanofiberous membrane for OA treatment.

Results

PCL-*g*-lignin copolymer. We grafted poly(ε-caprolactone) (PCL) with the hydroxyl groups of lignin via solvent-free ring-opening polymerization (ROP), in which PCL provides mechanical support and lignin serves as antioxidant agent (**Figure 2a**). Solvent-free polymerization is desirable as lignin is unable to dissolve in common organic solvents. The chemical structure of the PCL-*g*-lignin copolymer was

characterized via ^{1}H nuclear magnetic resonance (NMR) and Fourier transform infrared spectrum (FTIR). The NMR spectrum of lignin copolymer is shown in **Figure S1a**. In the ^{1}H NMR spectra (**Figure S1a**), the signals at 6.5–8.0 ppm can be attributed to aromatic H of lignin. While the signals at 3.5–4.0 ppm are assigned to H of the methoxyl groups of lignin. The characteristic ^{1}H NMR signals of PCL chains are located at 1.4, 1.6, 2.3 and 4.1 ppm. In addition, the signal of the end units of PCL chains (peak b) presents at 4.21 ppm, and the average PCL chain length in the copolymer is calculated as n = 23.5 repeat units (according to the area ratio of peak a/ b). Quantified by ^{31}P NMR, the aliphatic and hydroxyl OH group content of the PCL-g-lignin copolymer were 0.64 and 0.43 mmol/g (**Figure S2**), respectively. FTIR of lignin (**Figure S1b**) shows the peaks at ~3450 cm^{-1} corresponding to O–H stretching vibration, 2900 cm^{-1} corresponding to C–H stretching vibration, 1600 cm^{-1} and 1510 cm^{-1} attributable to aromatic ring vibrations of the phenyl propane skeleton. Typical FTIR bands of PCL chains are located at 2950 cm^{-1} (asymmetric stretching vibration of CH_2), 2860 cm^{-1} (symmetric stretching vibration of CH_2), 1730 cm^{-1} (carbonyl stretching vibration), 1290 cm^{-1} (C–O and C–C stretching vibrations), and 1240 cm^{-1} (asymmetric C–O–C stretching vibration). These results confirm the successful conjugation between PCL and lignin.

The molecular weight (Mn) of the PCL-*g*-lignin copolymer was characterized by gel permeation chromatography (GPC), yielding M_n = 12.0 kDa, M_w = 32.5 kDa, and dispersity index = 3.9. As Mn of unmodified lignin is 5 kDa, the mass percentage of lignin in the copolymer was determined to be 41.7%. The differential scanning

calorimeter (DSC) curve (**Figure S1c**) confirms that PCL-*g*-lignin is a semi-crystalline polymer, which displays a glass transition temperature (T_g) of 17 °C and a melting temperature (T_m) of 48 °C, with 44.4% crystallinity. It means that at body temperature (37 °C), the copolymer is in the rubber state, where the material is soft and flexible like rubber similar to the mechanical properties of cartilage tissue [35]. In addition, the copolymer is soluble in many organic solvents, which facilitates the subsequent processing.

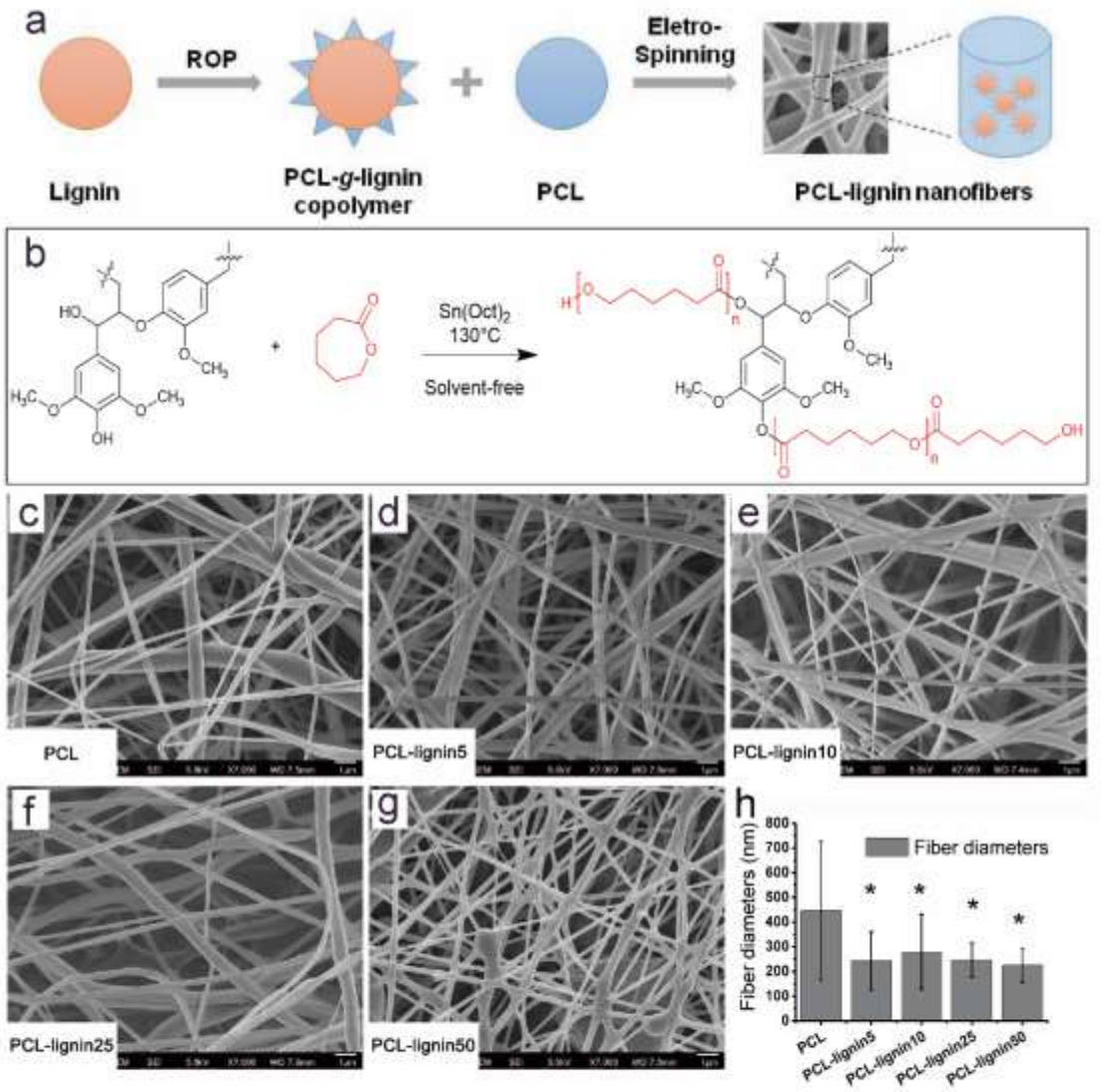

Nanofibers	PCL	PCL-lignin5	PCL-lignin10	PCL-lignin25	PCL-lignin50
(PCL : PCL-*g*-lignin)	100 : 0	95:5	90:10	75:25	50:50

Figure 2. (a) Schematic illustration of PCL-g-lignin and PCL-lignin nanofiers. (b) Synthetic route for PCL-*g*-lignin copolymers via solvent-free ring-opening polymerization (ROP). (c-g) Scanning Electron Microscopy (SEM) images of different nanofibers: PCL, PCL-lignin5, PCL-lignin10, PCL-lignin25, PCL-lignin50. The numbers indicate the weight percentage of lignin. (h) Fiber diameter. Data points represent as mean ± S.D. (n = 3). *$P < 0.05$.

Material characterization of PCL-lignin nanofibers. Electrospun nanofibers display a unique architecture mimicking the native extracellular matrix of human tissue, and they have been widely used in biomedical and tissue engineering applications [36]. As shown in **Figure 2c-h**, neat PCL fiber exhibited a large fiber diameter of 446 ± 280 nm, and the addition of lignin copolymer into PCL significantly reduced the fiber diameters down to 200 ~ 280 nm. All the lignin contained nanofibers showed similar fiber diameters (243 ± 118 nm for PCL-lignin5, 279 ± 152 for PCL-lignin10, 247 ± 69 for PCL-lignin25, 201 ± 52 for PCL-lignin40 and 224 ± 68 for PCL-lignin50). It is generally accepted that lignin can act as a reinforcing agent for polymer matrices[23, 34]. In the copolymer system, lignin provides high compressive stiffness while PCL offers rubbery property. As shown in **Figure 3a–3d**, higher PCL percentage (thus lower lignin content) offers better tensile property. PCL-lignin5 exhibits a tensile strength of 4.45 ± 0.26 MPa, a Young's modulus of 9.50 ± 1.0 MPa, and an elongation at breaking of 150% ± 19%. On the other hand, a high amount of lignin weakens the tensile strength, likely due to compromise of matrix integrity. PCL-lignin50 gives a tensile strength of 0.66 ± 0.13 MPa, Young's modulus of 3.30 ± 0.70 MPa, and elongation at breaking of 67% ± 4%.

Unmodified lignin is brittle and tends to aggregate in polymer matrix due to the π-π stacking of its aromatic rings and extreme polar surface[37]. Polymeric modification of lignin is considered as an effective approach to enhance the binding between lignin and polymer matrix and improve the performance of the resulting composites. In this study, we grafted PCL chains on the surface of lignin and improved the compatibility of lignin

and PCL nanofibers. It is reported that the interaction of the copolymers and the matrix could be a crucial factor for mechanical reinforcement[38], as the energy dispersion to lignin copolymer units can be well integrated in the PCL fibers through the strong entanglement among the grafted PCL chains and PCL matrix.

The viscoelastic properties of the nanofibers were analyzed by dynamic mechanical analysis (DMA) with temperature sweeping from 30 ºC to 60 ºC. The storage modulus G′, loss modulus G″, and tan(δ) are shown in **Figure 3e and Figure 3f**. The bare PCL nanofiber displays the lowest G′ (3.8–5.3 MPa) and G″ (0.25–0.39 MPa) values. With lignin, the copolymer enhanced the viscoelastic strength of the fibers. PCL-lignin5 exhibits the highest G′ (11.1–15.4 MPa) and G″ (0.93–1.43 MPa) values. The variation of G′ with the lignin percentage is consistent with the Young's modulus measurements(**Figure 3b**). The hyperbranched structure of PCL-*g*-lignin macromolecules which is capable of resisting intermolecular slippage accounts for the improvement of viscoelasticity.

Lignin is known for its excellent antioxidant property[39]. The antioxidant activities of the polymer nanofibers were assessed using 1,1-diphenyl-2-picrylhydrazyl (DPPH) assay. As shown in **Figure 3g**, a longer incubation time or a higher copolymer concentration leads to more inhibition of free radicals. IC50 (50% free radical inhibition) of the PCL-*g*-lignin copolymer is calculated to be 340 μg/mL with 0.5 h or 130 μg/mL with 1 h incubation (**Figure S1e**), suggesting that PCL-*g*-lignin copolymer has the antioxidant potency comparable to many commonly used antioxidants, such as vitamin

E (α-tocopherol, 380 μg/mL)[40], butylated hydroxytoluene (BHT, 290 μg/mL)[40], and honey (20–150 μg/mL)[41]. **Figure 3h** presents the free radical inhibition profiles of the PCL-lignin nanofibers. The bare PCL nanofiber exhibits the lowest free radical scavenging activity (<35% even after 48 h). In blank control （这个 controls 是什么材料？还是没有材料？如果是没有材料的话，我不知道你们怎么测的。还是删掉比较好，审稿人只需要文献证明即可） without any treatment, the free radical scavenging activity was 33.72% after 48h, close to PCL, indicating the decomposition of radicals automatically and bare PCL has little scavenging activity[42]. The antioxidant activity of PCL-lignin copolymer increases with increasing of lignin percentage. Among the nanofibers, PCL-lignin50 displays the highest inhibition of free radicals, which is 97.50% ± 1.30% after 48 h of incubation. In all the following experiments, PCL-lignin50 was used. We further analyzed capability of PCL-lignin50 to scavenge free radicals using two types of ROS asssy kit （什么 ROS 写清楚）. As shown in **Figure S3**, PCL-lignin50 showed 42.23% inhibition of superoxide anion after 30min and 32.29% inhibition of hydroxyl radical after 1h, much higher than PCL and PCL-VE.

FigS3 可以跟 Figure3 的 g，h 一起组合成 Figure4

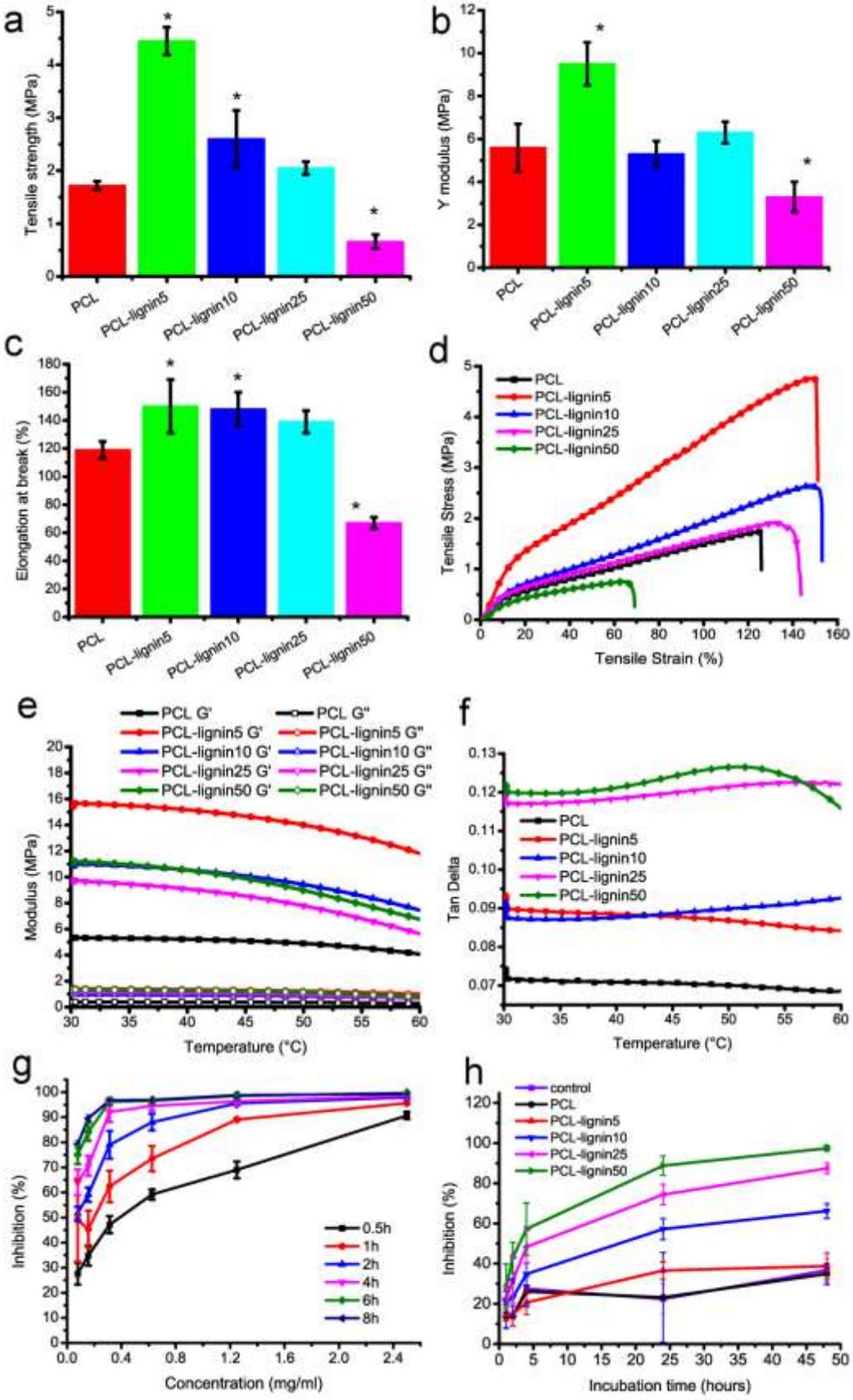
a
Tensile strength (MPa)
PCL
PCL-lignin5
PCL-lignin10
PCL-lignin25
PCL-lignin50
b
Y modulus (MPa)
c
Elongation at break (%)
d
Tensile Stress (MPa)
Tensile Strain (%)
e
PCL G'
PCL G"
PCL-lignin5 G'
PCL-lignin5 G"
PCL-lignin10 G'
PCL-lignin10 G"
PCL-lignin25 G'
PCL-lignin25 G"
PCL-lignin50 G'
PCL-lignin50 G"
Modulus (MPa)
Temperature (°C)
f
Tan Delta
Temperature (°C)
g
Inhibition (%)
0.5h
1h
2h
4h
6h
8h
Concentration (mg/ml)
h
control
Inhibition (%)
Incubation time (hours)

Figure 3. Characterization of PCL-lignin nanofibers. (a) Tensile strength. (b) Young's modulus. (c) Elongation at breaking point. (d) Stress-strain curves. (e) Storage (G′, solid symbols) and loss (G″, open symbols) moduli versus temperature as determined by DMA (1% strain and 1 Hz). (f) tan(δ). (g) Free radical inhibition of PCL-*g*-lignin copolymer with different incubation time determined by DPPH assay. (h) Free radical inhibition of PCL and PCL-lignin nanofibers. The numbers indicate the weight percentage of lignin. All data points represent mean ± S.D. (n = 3). **P* < 0.05.

我们需要把 Figure3 分成两个图 Fig3 和 Fig4，Figure3 是 a-f 主要讲力学和流变；Figure4 主要讲抗氧化。

PCL-lignin nanofibers improve cell viability of H_2O_2-stimulated human chondrocytes. Cell viability was analyzed using Cell Counting Kit-8 (CCK-8) assay. As shown in **Figure 4a**, all the lignin-containing nanofibers showed higher cell viability as compared to PCL nanofiber, demonstrating their good biocompatibility[43]. The cells on PCL-lignin50 exhibited the highest viability (82.95%) and proliferation rate among all PCL-lignin nanofibers. Therefore PCL-lignin50 nanofibers were selected for the following cell and animal study due to its advanced antioxidant properties and biocompatibility.

The viability of human chondrocytes on the nanofibers of PCL, PCL containing 20% vitamin E (PCL-VE), and PCL-lignin50 (~20% lignin) with or without H_2O_2 exposure (24 h) was reported by CCK-8 assay. As shown in **Figure 4b**, the chondrocytes viability were 69.72% in PCL, 77.50% in PCL-VE and 82.95% in PCL-lignin50 nanofibers. However, H_2O_2 treatment significantly decreased the cell viability to 25.33% in PCL,

40.65% in PCL-VE and 58.70% in PCL-lignin50, in which PCL-lignin50 was most effective to reverse the oxidative stress imposed by H_2O_2. These results were further confirmed by the live/dead assay, which determines cell viability based on plasma membrane integrity and esterase activity [44]. As revealed by confocal imaging(**Figure 4c**）, H_2O_2 treatment led to the decrease of live cells (green) and the increase of dead cells (red). Compared to PCL (43.10%) and PCL-VE (64.46%), PCL-lignin50 ensured the highest live cell ratio of 81.08% under the challenge by H_2O_2 (**Figure 4d and 4e**). We also evaluated the levels of apoptotic chondrocytes on different nanofibers by flow cytometry shown in **Figure 4f**. Consistently, PCL-lignin50 most effectively suppressed the cell apoptosis induced by H_2O_2, which decreased only 6.70%, less than PCL (a 40.30% decrease) and PCL-VE (a 24.30% decrease). Taken together, PCL-lignin50 effectively protects chondrocytes from oxidative stress.

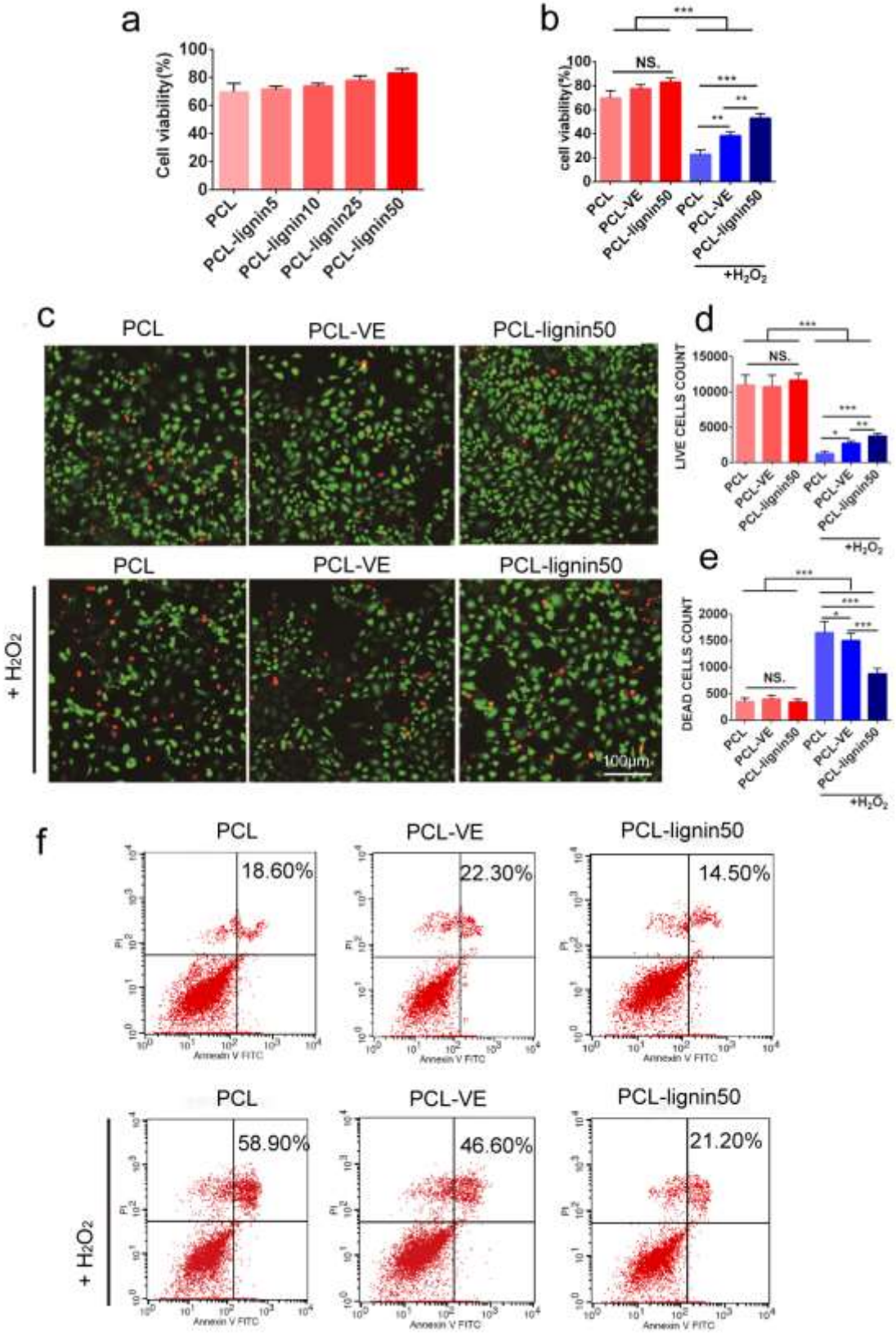

Figure 4. Effects of PCL-lignin50 nanofibers on cell viability of H_2O_2-induced chondrocytes. (a) Cell viability on PCL, PCL-lignin nanofibers detected by CCK-8

assay. (b) Cell viability on PCL, PCL-VE, PCL-lignin50 after treatment with or without H_2O_2 detected by CCK-8 assay. (c) Confocal imaging of live (green) and dead (red) cells with or without H_2O_2 exposure. Quantification of live cells (d) and dead cells (e) with or without H_2O_2 exposure. (f) Cell apoptosis detection by a flow cytometer after treatment with or without H_2O_2 for 24 h (n = 3). All data represent mean ± S.D. (n = 3). *** $P < 0.001$, ** $P < 0.01$, * $P < 0.05$.

Inhibition of inflammatory factor expression by PCL-lignin50 nanofibers. Matrix metalloproteinase 13 (MMP-13) plays a key role in OA pathogenesis, which degrades the collagen network in cartilage by cleaving type II collagen[45]. Here immunofluorescence staining was used to analyze MMP-13 level in H_2O_2 stimulated chondrocytes on the nanofibers to evaluate ECM degradation in the early stage of OA, with the intensity of fluorenscence correlated with inflammation. As shown in **Figure 5a**, the intensity of MMP-13 positive staining decreased in the order of PCL, PCL-VE, and PCL-lignin50 after treatment of H_2O_2, indicating the increased alleviation of ECM degradation induced by H_2O_2. Mostly negative staining of MMP-13 was found in PCL-lignin50+H_2O_2 group, demonstrating the strong antioxidant activity of PCL-lignin50 to suppress the inflammatory factors. This finding was further corroborated by real-time polymerase chain reaction (qRT-PCR) analysis (**Figure 5b**). H_2O_2 treatment increased the expression of inflammatory factors (MMP-13, IL-6 and IL-1β), but the increase was lessened by PCL-VE and PCL-lignin50. PCL-lignin50 nanofibers down-regulated the expression of the inflammatory factors by 62.50%, 48.67%, and 28.68%, respectively,

compared to PCL. The results testify that PCL-lignin50 nanofibers are able to effectively prevent H_2O_2-induced inflammation in chondrocytes.

H_2O_2-induced oxidative stress suppressed by PCL-lignin50 nanofibers. The antioxidant perform of PCL-lignin50 was further investigated by qRT-PCR analysis to assess the expression of antioxidant factors including *SOD*, *CAT*, *GSH-PX*, and *NRF-2*. As shown in **Figure 5c**, chondrocytes on PCL-lignin50 nanofibers and subjected to H_2O_2 stimulation exhibited significant increase in the expression of antioxidant factors including *SOD*, *CAT*, *GSH-PX*, and *NRF-2*, as compared to the cells grown on PCL and PCL-VE nanofibers.

Intracellular ROS generation induced by H_2O_2 was determined by performing flow cytometry analysis using dichloro-dihydro-fluorescein diacetate (DCFH-DA) as the probe. DCFH-DA can freely cross the cell membrane, and be hydrolyzed by the intracellular esterase to generate dichlorofluorescin(DCFH), which is then oxidized by intracellular ROS to produce fluorescent dichlorofluorescein (DCF). As shown in **Figure 5d**, H_2O_2 prominently induced increase of intracellular ROS in chondrocytes. Notably, only 42.80% of the cells were on PCL-lignin50 nanofibers were stained with DCF, much lower than the cells on PCL-VE (66.70%) and PCL (77.48%) nanofibers. These results show that PCL-lignin50 nanofibers are able to restrain ROS generation (thus the consequent cellular damages) in chondrocytes under oxidative stress.

Furthermore, we examined the activity of antioxidant factors (SOD, CAT) and levels of GSH and MDA (lipid peroxidation product) in H_2O_2-stimulated chondrocytes. As

shown in **Figure 5e**, the SOD, CAT activities and the GSH level were increased markedly while the MDA level was down-regulated. PCL-lignin50 increased the activity of SOD and CAT as well as GSH level by 86.70%, 35.30%, and 71.40%, respectively. These effects are much more significant than that from PCL. Meanwhile, PCL-lignin50 decreased the MDA level by 42.60%. The results indicate that PCL-lignin50 nanofibers are able to assist chondrocytes to resist oxidative stress.

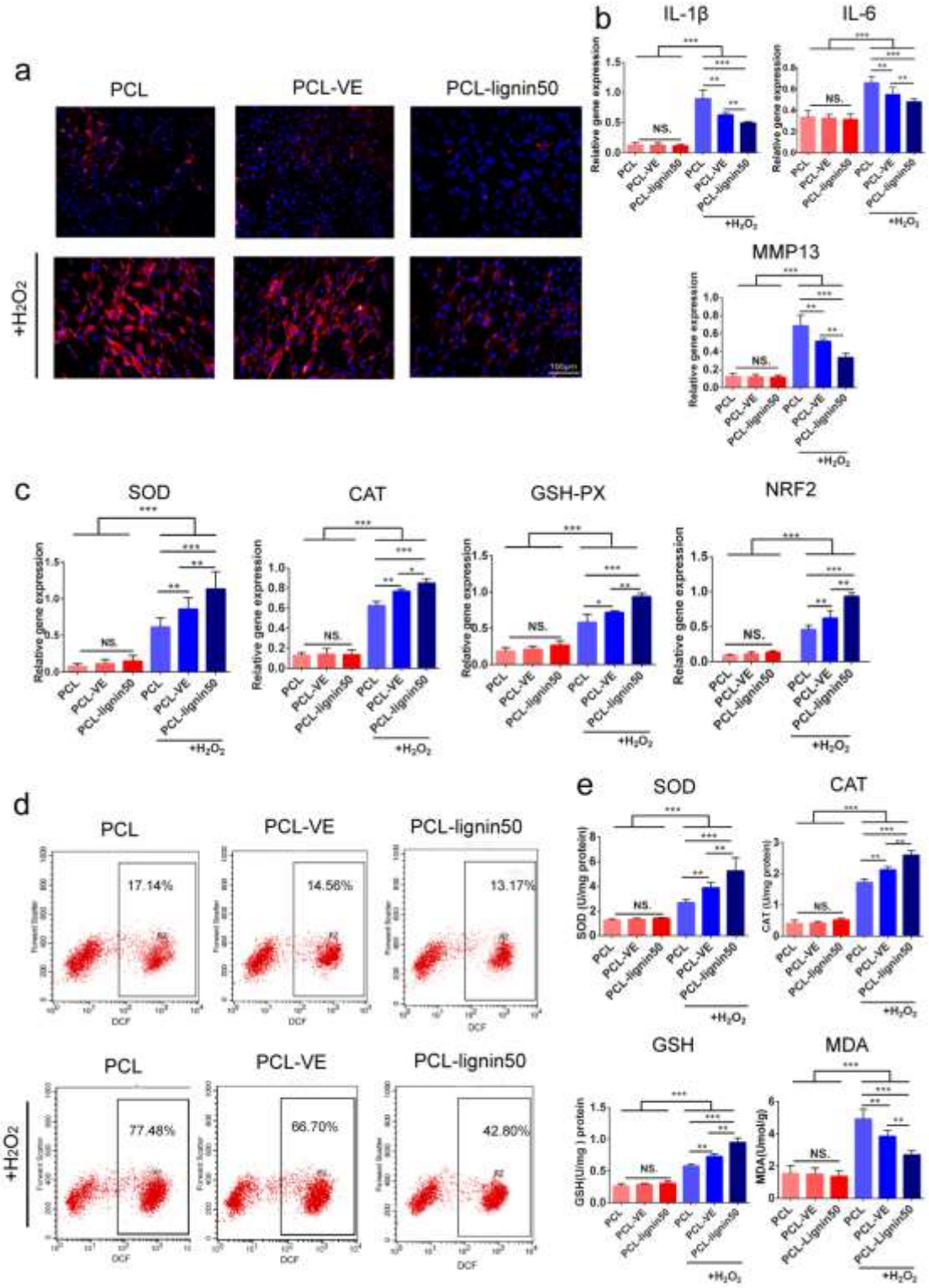

Figure 5. Inhibition of inflammatory factors and suppression of H_2O_2-induced oxidative stress by PCL-lignin50 nanofibers. (a) Immunofluorescence staining for MMP-13 in chondrocytes cultured on the nanofibers with or without H_2O_2 treatment. qRT-PCR detection of (b) inflammatory factors *IL-1β*, *IL-6*, and *MMP-13* and (c)

antioxidant factors *SOD*, *CAT*, *GSH-PX*, and *NRF2* in chondrocytes cultured on the nanofibers. (d) Intracellular ROS detection with DCFH-DA obtained by flow cytometry. (e) Determination of antioxidant enzymes SOD, CAT, and MDA. All data represent mean ± S.D. (n = 3). *** $P < 0.001$, ** $P < 0.01$, * $P < 0.05$.

Autophagy activation by PCL-lignin50 nanofibers. Autophagy is an intracellular catabolic mechanism that could protect chondrocytes from excessive oxidative stress in OA[46]. Autophagosome formation as an indication of autophagy was evaluated by transmission electron microscopy (TEM). As shown in **Figure 6a**, fewer autophagic vacuoles were present without H_2O_2 treatment. After exposure to H_2O_2 for 24 h, the human chondrocytes on PCL-lignin50 nanofibers produced more cytoplasmic vesicles with characteristic single-membrane structure of autolysosome (**Figure 6b**). Cells on PCL-VE also showed a certain amount of autophagosomes, whereas those on PCL exhibited few autophagosomes similar to the case without H_2O_2 treatment. To further confirm the ability of PCL-lignin50 to trigger autophagy, chondrocytes were transiently transfected with GFP-LC3B (an autophagosome marker) and observed under a fluorescence microscope (**Figure 6c**). It was found that more green fluorescence spots were present in the cytoplasm of the chondrocytes on PCL-lignin50 nanofibers than those on PCL and PCL-VE (**Figure 6d**). Autophagy is known to be cytoprotective in chondrocytes, relative to chondrocyte hypertrophy. As observed in Figure 6c, there's no obvious change of cell morphology in all the groups, possibly due to the early stage of hypertrophy. But more autophagic vacuoles (autophagosomes) as marked by yellow

were observed in chondrocytes cultured on PCL-lignin50 with the treatment of H_2O_2. In addition, the expression levels of autophagy markers (*ATG4*, *ATG7*, *Keap1* and *P62*) were evaluated as evidenced by qRT-PCR analysis (**Figure 6e - 6h**). In contrast to PCL, PCL-lignin50 significantly up-regulated the expression levels of *ATG4* and *ATG7* and suppressed the expression of *Keap1* and *P62*, which negatively regulate Nrf2 signaling pathway in selective autophagy under oxidative stress. These findings suggest that PCL-lignin50 can suppress H_2O_2-induced oxidative stress through autophagy activation.

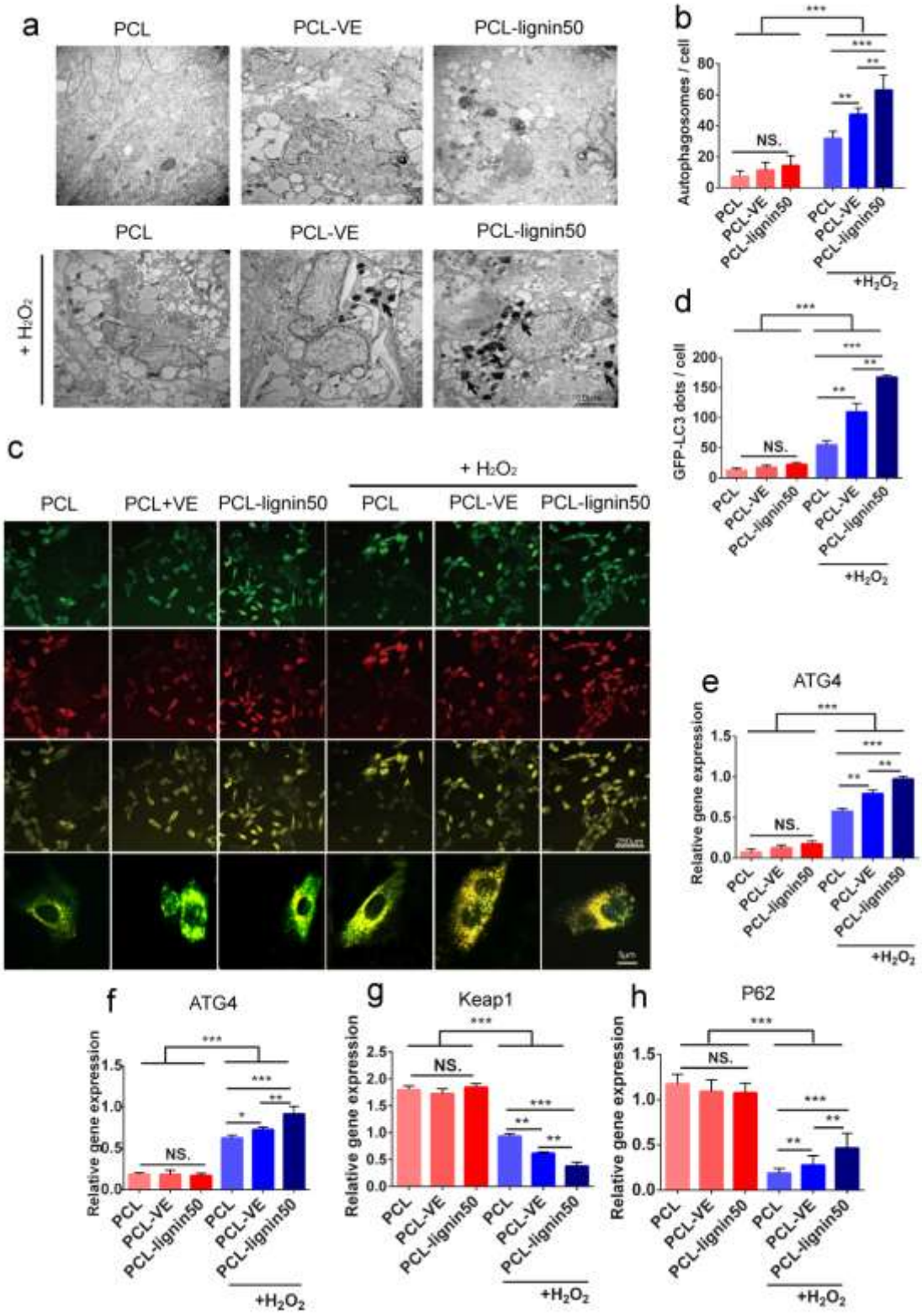

Figure 6. Autophagy activation by PCL-lignin50 nanofibers to protect chondrocytes from H_2O_2-induced oxidative stress. (a) TEM images of autophagic vesicles and autophagosomes in chondrocytes. The black dots marked by black arrows

indicate autolysosomes. (b) Quantification of autophagosomes in chondrocytes. (c, d) Quantification and fluorescence microscopy observation of GFP-LC3B in chondrocytes after treatment with 0.4 mM H_2O_2 for 24 h. (e-h) qRT-PCR detection of expression levels of autophagy markers *ATG4*, *ATG7*, *Keap1* and *p62*. All data represent mean ± S.D. (n = 3). *** $P < 0.001$, ** $P < 0.01$, * $P < 0.05$.

PCL-lignin50 nanofibers attenuate OA progression *in vivo*. To investigate the *in vivo* degradation of PCL-lignin50, lignin concentration in the synovial fluid was tested after implantation of nanofibrous membrane on the joint surface through a minimally invasive surgery based on a papain-induced rabbit model. As shown in **Figure 7a,** residual PCL-lignin50 still remained on the surface of articular joint after 10 days. Intra-articular lignin content with PCL-lignin50 nanofiber treatment was higher at day 10 than that at day 0. And lignin content of PCL-lignin50 injection was 3.4 folds higher than treatment with lignin injection at day 10 (**Figure 7b**). The results demonstrated the sustained release of lignin with the gradual degradation of PCL-lignin50 after implantation.

Further, we implanted PCL, PCL-VE and PCL-lignin50 nanofiberous membrane to replace the damaged cartilage tissue of OA rabbit for four weeks. Macroscopic observation of the knee joints showed (**Figure 7c**) that PCL-lignin50 treatment had no adverse effect on cartilage. The smooth and glistening surface of the joint is similar to that in the sham-operated group. OA characteristics, such as erosion and large lesions, were observed in the untreated group and the group treated with PCL membrane. The

cartilage lesion in the group treated with PCL-VE membrane was also obvious. The cartilages received the treatment of PCL-lignin50 nanofiberous membrane looked similar to the normal cartilage. PCL-lignin50 had strong antioxidant properties and scavenging effect on reactive oxygen, protecting the cartilage and providing an excellent repair environment for normal chondrocytes in the cell matrix. With the eliminating of reactive oxygen and suppression of the inflammatory factors (such as IL-1beta, IL-6), damaged cartilage was alleviated, beneficial to the regeneration of healthy chondrocytes. With the apoptosis of injured chondrocytes and the renewal of newborn cells, partial cartilage was regenerated [3, 15]. These observations were quantified by Macroscopic Score, a standard for evaluation of cartilage damage (**Figure 7e**). The OA joints administered with PCL-lignin50 nanofiberous membrane showed the lowest score (6.68 ± 0.51) among all the treatment groups, with a 47.57% decrease as compared with the untreated group.

Histological analyses by Hematoxylin and eosin (HE), safranin O-fast green, toluidine blue, and Alcian blue staining were performed to determine cartilage damage. As shown in **Figure 7d**, the cartilage samples from the sham-operated and PCL-lignin50 treatment group appear normal, while those from the untreated and PCL treatment groups exhibit pronounced morphological changes, including fissures and fibrillation, increase of tissue cellularity with cloning, and loss of glycosaminoglycan (GAG). In addition, the Osteoarthritis Research Society International (OARSI) Score was used to assess cartilage degeneration and damage (**Figure 7f**). The OARSI Score of PCL-lignin50 treatment group (9.66 ± 0.52) is the lowest among all the treatment groups and

shows no significant difference to that of the untreated group.

Furthermore, we examined the antioxidant enzyme activity of SOD and the level of MDA in the synovial fluid to determine whether PCL-lignin50 could inhibit oxidative stress in OA joints. As shown in **Figure 7g-7h**, the SOD activity decreased and the MDA level elevated in the untreated group, indicating that papain caused oxidative stress damage. And PCL treatment did not help. On the other hand, PCL-lignin50 treatment significantly improved the SOD activity by 62.28% and reduced the MDA level by 48.36%. The protein expression levels of inflammatory factors (*MMP-13* and *IL-6*) in the synovial fluid were also detected by enzyme-linked immunosorbent assay (ELISA) (**Figure 7i-7j**). The expression of *MMP-13* and *IL-6* was enhanced remarkably after papain treatment. PCL-lignin50 treatment significantly reduced the levels of *MMP-13* and *IL-6* by 52.28% and 63.20%, respectively.

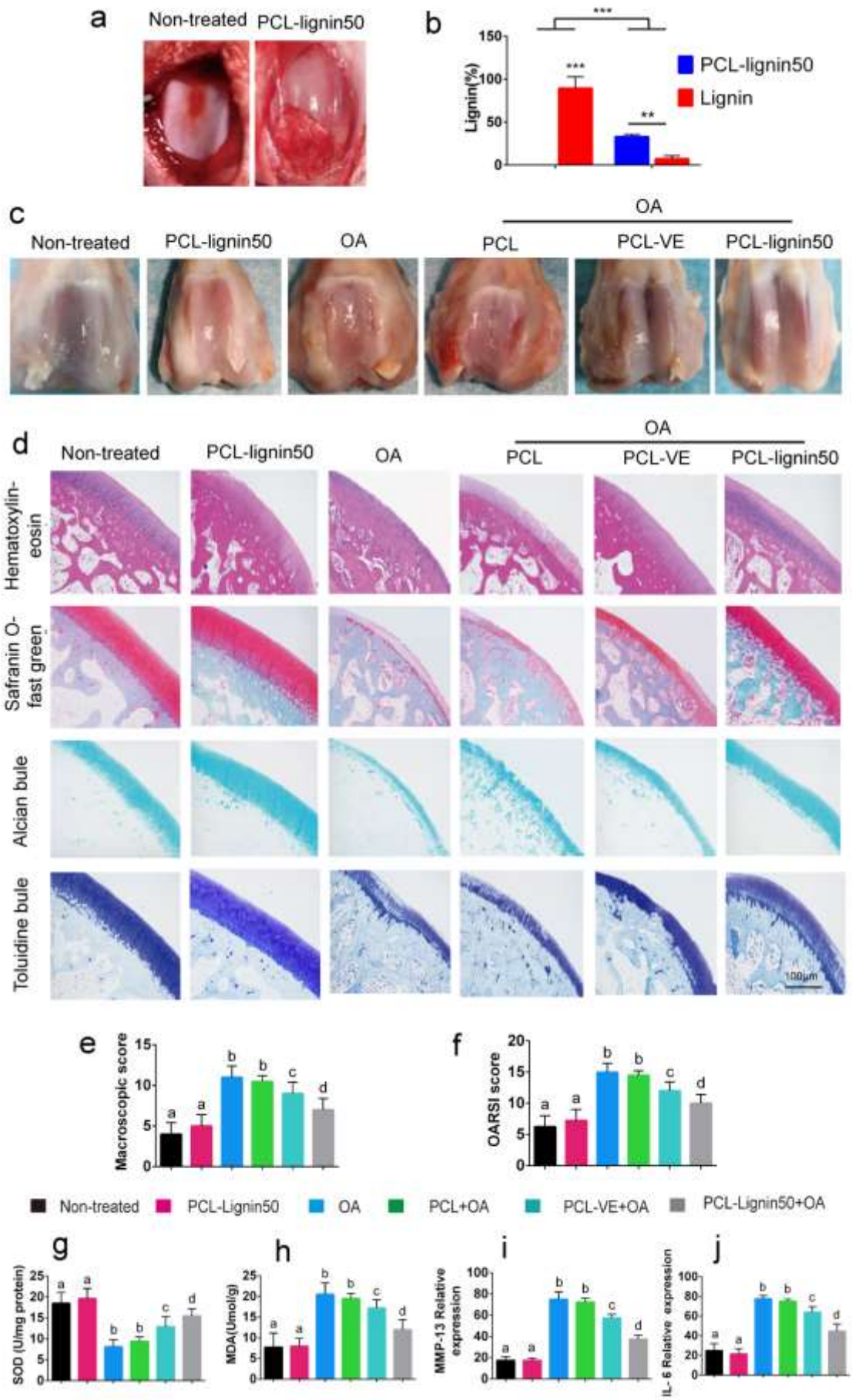
a
Non-treated
PCL-lignin50
b
Lignin(%)
PCL-lignin50
Lignin
c
Non-treated
PCL-lignin50
OA
OA
PCL
PCL-VE
PCL-lignin50
d
Non-treated
PCL-lignin50
OA
OA
PCL
PCL-VE
PCL-lignin50
Hematoxylin-eosin
Safranin O-fast green
Alcian bule
Toluidine bule
100μm
e
Macroscopic score
f
OARSI score
Non-treated
PCL-Lignin50
OA
PCL+OA
PCL-VE+OA
PCL-Lignin50+OA
g
SOD (U/mg protein)
h
MDA(Umol/g)
i
MMP-13 Relative expression
j
IL-6 Relative expression

Figure 7. Attenuation of OA progression by PCL-lignin50 nanofibers *in vivo*. (a) Macroscopic observation of implanted PCL-lignin membrane in the joint for 10 days. (b) Intra-articular lignin concentration in the synovial fluid was tested after implantation of nanofibrous membrane on the joint surface for 10 days. (c) Macroscopic observations. (d) HE, safranin O-fast green, Alcian blue, and toluidine blue staining to evaluate degeneration and damage. (e) Macroscopic Score and (f) OARSI Score of OA joints to evaluate of cartilage degeneration and damage after PCL-lignin membrane therapy for 4 weeks. (g, h) The antioxidant enzyme activity of SOD and level of MDA in the joint fluid were determined by assay kits. (i, j) The protein expression levels of inflammatory factors (MMP-13 and IL-6) in the synovial fluid were detected by ELISA. All data represent mean ± S.D. (n = 3). Different letters shows $P < 0.05$ and the same letter shows $P \geqslant 0.05$.

Discussion

Here we report a novel strategy for OA therapy, whose working mechanism and effectiveness are carefully verified both in vitro (human chondrocyte) and in vivo (a rabbit OA model). In contrast to the conventional injection of antioxidants which suffer from quick clearance, we exploit the intrinsic and durable antioxidant activity of lignin and fabricate implantable nanofibrous membrane by electrospinning nanofibers of PCL-*g*-lignin copolymer for OA treatment.

PCL-*g*-lignin copolymer is synthesized by grafting PCL with the hydroxyl groups of lignin via solvent-free ring-opening polymerization. We demonstrate that the copolymer is biocompatible and biodegradable. Its antioxidant potency and mechanical properties can be tailored by varying the ratio between PCL and lignin. In OA joints,

the excessive oxidative stress is the main cause to tissue damage [5, 9, 10]. We demonstrate that antioxidant PCL-lignin nanofibers relieve such problem by increasing cell viability and reducing apoptosis, attenuating inflammation, suppressing ROS, activating antioxidant enzymes, activating autophagy, and activating Keap1-Nrf2 axis. Keap1-Nrf2 system is important in preventing oxidative injure by increasing the expression of antioxidant enzymes in chondrocytes under oxidative stress[47, 48]. Under quiescent conditions, the transcription factor Nrf2 is degraded by its binding partner Keap1 that is an adaptor of the ubiquitin ligase complex[20, 49]. Under oxidative stress, p62 phosphorylates and interacts with the Nrf2-binding site of Keap1 and competitively inhibits the Keap1-Nrf2 interaction via autophagy, leading to the upregulation of the expression genes encoding antioxidant and anti-inflammatory factor[5, 50]. Our study suggests that PCL-lignin50 alleviates oxidative stress by activating autophagy responsive Nrf2 through Keap1 suppression during OA progression.

It has been widely accepted that excessive ROS produced by injured chondrocytes contribute to OA progression and that inhibiting them can impede the pathological process[5, 9]. In this study, we fabricated implantable and degradable antioxidant PCL-lignin nanofiber membrane for effective osteoarthritis treatment. Peroxidation products and oxidation enzymes such as ROS, MDA increased after papain indluced injury, which leads to increased cellular apoptosis and upregulation of catabolic markers[10]. PCL-lignin nanofibers reduced inflammatory factor (*IL-6*, and *MMP-13*) and activated antioxidant enzymes. Furthermore, PCL-lignin nanofibers can effectively suppress OA

development and cartilage degradation, as evidenced by the *in vivo* macroscopic and histological evaluations. This study shall provide a novel strategy for arthroscopic intervention of OA therapy using such implantable and biodegradable scaffolds with intrinsic and sustained antioxidant activities.

Antioxidants such as polysaccharides, vitamin E, vitamin C are conventionally employed to treat OA[13, 15]. Typically, intra-articular injection to OA knee once a week for more than 8 weeks is required[15, 51]. But effectiveness is largely limited fast clearance and degradation of drug molecules. For oral therapy, patients usually take vitamin E (100−300 mg/day) or resveratrol (40mg, two times per day) for at least 6 months[14]. But such systemic administrate gives very low drug bioavailability at the joints[52]. In addition, high dosage required by the conventionally treatment may cause systemic side-effects[52, 53]. Conventional treatment typically offers only 25%~31% decrease of OARSI score (standard histological grading system for qualitative description of various cartilage characteristics) by after 4 weeks treatment[14, 54]. In our study, PCL-lignin nanofiber membrane reduced the OARSI score by 40.49% without the need of repeated injection and systemic side-effects. In conclusion, the novel antioxidant nanofibrous membrane of PCL-lignin is capable of inhibiting ROS generation by autophagic activation and postulates the potential of arthroscopic implantation of antioxidant biomaterials for OA therapy.

Methods

Synthesis and characterization of PCL grafted lignin copolymers

PCL-*g*-lignin copolymer was synthesized via ring-opening polymerization. Here we used solvent-free polymerization, as kraft lignin is insoluble in water (neutral) or many organic solvents, but only soluble in alkaline solution (pH > 12). 2 g of lignin (Sigma-Aldrich, Alkali, M_n = 5 kDa, dried at 105 °C prior to use) and 8 g of ε-caprolactone were mixed in a round-bottom flask and purged with N_2. After that, Tin(II) 2-ethylhexanoate as a catalyst (0.5 wt% of monomer) was dropped into the flask, and mixed at 130 °C for 24 h. The mixture was then dissolved in chloroform and precipitated into an excess amount of diethyl ether. The PCL-*g*-lignin copolymer was harvested and dried at 50 °C for further characterization. The polymerization degree of the copolymer is 61.4 (by NMR and GPC).

The chemical structure of the PCL-*g*-lignin copolymer was characterized via ^{1}H nuclear magnetic resonance (JEOL 500 MHz) with $CDCl_3$ as a solvent[55] and a FTIR (Spectrum 2000, Perkin Elmer, USA)[56]. The molecular weight of the copolymer was characterized via Waters GPC (SCL-10A and LC-8A, Shimadzu, Japan equipped with two Phenogel 5 mm 50 and 1000 Å columns in series and a Shimadzu RID-10A refractive index detector) by using HPLC tetrahydrofuran as an eluent. The flow rate of tetrahydrofuran eluent was 1.0 mL/min at 25 °C. The number average molecular weights (M_n), weight average molecular weights (M_w) and polydispersity index (PDI, M_w/M_n) were determined with a calibration based on linear poly(methyl methacrylate) standards. The thermal properties of the copolymer were assessed using a dynamic

stability control (DSC)(TA Instruments Q100, USA)[57]. The following protocol was used for each sample: heating from -80 °C to +150 °C at 20 °C/min, holding at +150 °C from 5 min, cooling from +150 °C to -80 °C at 20 °C/min, and finally reheating from -80 to +150 °C at 20 °C/min.

Electrospinning and characterization of nanofibers

PCL (Sigma-Aldrich, M_n = 80 kDa) and the PCL-*g*-lignin copolymer were mixed in different ratios (95:5, 90:10, 75:25, 50:50). The solvent used was 1, 1, 1, 3, 3, 3-hexafluoro-2-propanol, and the total concentration of the solution was 8 wt%. Each solution was transferred into a syringe with a 25-gauge needle. The flow rate was set as 0.8 mL/h with voltage of 12 kV. The number in the sample code (such as the 25 in PCL-lignin 25) is the weight percentage of PCL-lignin in the system. The obtained fibers were dried overnight in a vacuum oven and used for further evaluations. Neat PCL and PCL-VE (PCL with 20% vitamin E) were prepared under the same conditions to serve as control groups.

Scanning Electron Microscopy (SEM)

Fibers were sputter-coated with thin layers of gold, and the surface morphologies were examined by SEM (JSM6700F, JEOL, Japan)[58]. For nanofibers, the average pore size was measured from 50 random fibers based on the SEM images by using Image J software (NIH, USA).

Tensile testing and viscoelastic behavior

For tensile testing, fiber mats (thickness ~ 100 μm) were prepared as rectangles with dimensions of 5 × 30 mm with the support of a paper frame[59]. The test was performed by a uniaxial tensile testing technique[60] (Instron 5942, USA). The gauge length was set as 20 mm, and the tensile rate was 10 mm/min. At least six samples were tested for each composition. The viscoelastic properties of the nanofibers were characterized by using DMA (Q800, TA Instrument, USA) with tension film model. The test was performed by ramping the temperature from 30 ºC to 60 ºC with a rate of 3 ºC per minute. The oscillating amplitude was 1% with the frequency of 1 Hz.

Determining Antioxidant activity

A DPPH assay was used to evaluate the antioxidant activity of the PCL-*g*-lignin copolymer and its nanofibers. For the copolymer, PCL-*g*-lignin was added to a series of glass vials, followed by the addition of 60 μM DPPH/MeOH solution in each vial. The DPPH free radical content was measured by checking the absorbance (517 nm) after incubation. For the nanofibers, 20 mg of each fiber was soaked in 20 mL of DPPH/MeOH solution, and the absorbance of DPPH supernatant was monitoredat each time point. The antioxidant activity was calculated as % indicating the inhibition of free radicals by detecting the absorbance changes compared to control. The scavenging types of ROS by PCL-lignin50 were further measured using superoxide anion assay kit (Solarbio, China) and hydroxyl radical assay kit (Solarbio, China), respectively. According to the manufacture's instructions, superoxide anion was assessed after 0.5h and hydroxyl radical was detected after 1h.

Chondrocyte culture

The human chondrocyte cell line (TC28a2) was purchased from ATCC (Rockville, MD, USA). The chondrocytes were cultured in high-glucose Dulbecco's modified Eagle's medium (DMEM, Gibco, USA) containing 10% fetal bovine serum (Gibco, USA) and 1% penicillin/streptomycin (Solarbio, China) in a 5% CO_2 humidified atmosphere at 37 °C. The culture medium was changed every other day.

H_2O_2-induced chondrocytes and treatment

Six groups were prepared: the chondrocytes were pre-seeded on PCL, PCL-VE and PCL-lignin nanofibers with or without 0.4 mmol/L H_2O_2 for 24 h, and the groups were designated as (1) PCL, (2) PCL-VE, (3) PCL-lignin50, (4) PCL+H_2O_2, (5) PCL-VE+H_2O_2, and (6) PCL-lignin50 +H_2O_2. Prior to cell seeding, the nanofibers were molded into circles (diameter = 14 mm). The nanofibers were sterilized in 75% ethanol for 2 h and then rinsed with phosphate buffer saline (PBS) containing 1% penicillin-streptomycin. The dried samples were irradiated by ultraviolet light overnight for sterilization. Approximately 8×10^4 chondrocytes were seeded on each nanofiber. The PCL-lignin50 nanofibers with the lowest cytotoxicity and highest antioxidative activity were chosen for further study.

Cell viability and apoptosis assay

The cytotoxicity and proliferation of cells on the PCL, PCL-VE, and PCL-lignin nanofibers were tested using a CCK-8 kit (Dojindo, Japan). Live/dead assays was performed by using a live/dead viability assay kit (Invitrogen, USA). Briefly, the cells

were incubated in a solution containing fluorescein diacetate (5 μM)/propidium iodide (20 μM) for 5 min at 37 °C in the dark. Then, the chondrocytes were counted and imaged using the High Content Screening (HCS) Platform (CX51110, Thermo Fisher Scientific, USA). The cell apoptosis was measured using an Annexin V-FITC/PI Apoptosis Detection Kit (KeyGEN, China) and analyzed by using a flow cytometer (BD Biosciences, USA).

Measurement of SOD, CAT, GSH, and MDA

The activities of antioxidant enzymes SOD, CAT, GSH, and MDA in the cell homogenate were examined by using SOD, CAT, GSH, and MDA assay kits (NanJing JianCheng Bio Inst, Nanjing, China), respectively, according to the instructions provided by the manufacturer.

Intracellular ROS detection

The intracellular ROS level was analyzed by using an ROS Assay Kit (Beyotime, Shanghai, China). After treatment with or without H_2O_2 for 24 h, human chondrocytes on PCL, PCL-VE, and PCL-lignin50 nanofibers were incubated with 10 μM DCFH-DA at 37 °C for 1 h in the dark. After washed with PBS three times, the cells were trypsinized and collected. The intracellular ROS level was measured by flow cytometry (ex/em 488 nm and 525 nm).

Immunofluorescence

The secretion of MMP-13 was detected by immunofluorescence. After cultured for 24 h, the samples were fixed with 4% formalin for 20 min and permeabilized with 0.3% Triton X-100 (W/V) in PBS for 10 min. After blocked by 5% BSA for 15 min at 25 °C, the primary antibody of MMP-13 (1:200 dilution, Abcam, USA) was added and incubated at 4 °C over night, followed by the incubation of the secondary antibody IgG-CY3 (1:100 dilution, BOSTER, China) for 2 h in the dark. The images were captured by an Olympus fluorescence microscope (BX53, Olympus, Japan).

Identification of autophagic cells

For autophagy assessment, the pre-transfected chondrocytes with a Premo™ Autophagy Sensor LC3B-GFP (BacMam 2.0m, Thermo Fisher Scientific, USA). After cultured for 24 h, the transfected cells were digested using 0.25% trypsin and seeded on PCL, PCL-VE, and PCL-lignin nanofibers followed by treatment with or without 0.4 mM H_2O_2 for 24 h. The chondrocytes were then fixed in 4% paraformaldehyde for 30 min at 4 °C and observed by a fluorescence microscope (Eclipse Ti-SR, Nikon, Japan), and the dots of LC3B-GFP were counted. Cells with more than 20 GFP-LC3 dots were defined as autophagic[61, 62]and were calculated by using the HCS platform.

For the TEM studies, chondrocytes were seeded on PCL, PCL-VE, and PCL-lignin nanofibers with or without 0.4 mM H_2O_2 for 24 h and then harvested. After washed with PBS twice, the samples were fixed with 2.5% glutaraldehyde and then treated by 1% osmic acid. After washed with PBS three times and subsequent dehydration, the samples were embedded in paraffin and cut into 70-nm sections by an ultra-thin slicing

machine (Leica EM UC6, Germany). After stained with uranyl acetate-lead citric, the specimens were observed by TEM (JEM1230, JEOL, Japan).

RNA extraction and qRT-PCR

The gene expressions of *IL-1β*, *IL-6*, *MMP-13*, *SOD*, *CAT*, *GSH-PX*, *NRF2*, *ATG4*, *ATG7*,*Keap1* and *p62* were analyzed by qRT-PCR. The total RNA was extracted using a HiPure Total RNA Mini Kit (Magen, China). Approximately 1000 ng of total RNA was extracted. The RNA transcription and qRT-PCR reactions were performed as described previously[63]. The designed primers are listed in **Table 1**. The relative gene expression levels were calculated by the $2^{-\Delta\Delta Ct}$ method using β-actin as a control. Each gene was analyzed in triplicate to reduce randomization error.

Table 1. Primers for RT-PCR performance.

gene	Forward primer（5'-3')	Reverse primer (5'-3')
MMP-13	GCCATTACCAGTCTCCGAGG	TACGGTTGGGAAGTTCTGGC
Il-6	CTCAATATTAGAGTCTCAACCCCCA	GAGAAGGCAACTGGACCGAA
IL-1β	CAGAAGTACCTGAGCTCGCC	AGATTCGTAGCTGGATGCCG
SOD	ACAAAGATGGTGTGGCCGAT	AACGACTTCCAGCGTTTCCT
CAT	AGTGATCGGGGGATTCCAGA	GAGGGGTACTTTCCTGTGGC
GSH-PX	GAACCGTTCGCGGAGGAAAG	AGAGCGTGAATGGGGCATAG
ATG4	CTCATCTACCTGGACCCCCA	AGAATCTAGGGACAGGTTCAGGA
ATG5	GGGTCCCTCTTGGGGTACAT	ACCACACATCTCGAAGCACA
ATG7	TGGTTACAAGCTTGGCTGCT	TCAAGAACCTGGTGAGGCAC
P62	GGTCGCGCTCACCTTTCT	TCCTTTCTCAAGCCCCATGTT
β-actin	CCCATCTATGAGGGTTACGC	TTTAATGTCACGCACGATTTC

OA animal model and treatment with PCL-lignin nanofibers

A total of 30 male New Zealand rabbits (Guangxi Medical University, Nanning, China) weighing 4.50 ± 0.2 kg were studied *in vivo*. All the experiments were conducted

according to the guidelines of the Animal Research Ethics Committee of the Guangxi Medical University (Protocol Number: 2017-6-27). OA was induced in the right knees of the rabbits by intra-articular injections of 500 μL 4% papain solution[64]. All of the animals were injected once weekly for 4 weeks[65, 66]. For nanofiber treatment, each right knee joint was opened via a medial parapatellar approach under anesthesia performed by injection of 0.1% pentobarbital sodium (40 mg/kg). The nanofibers were cover on the knee joints completely. Six different groups were examined: (1) sham-operated with no treatment, (2) sham-operated treated with PCL-lignin nanofibers (3) OA injected with 0.3 mL normal saline, (4) OA treated with PCL nanofibers, (5) OA treated with PCL-VE nanofibers, and (6) OA treated with PCL-lignin nanofibers. After four weeks of therapy, the New Zealand rabbits were euthanized and sacrificed. The joints were harvested for further examination.

Analysis of *in vivo* degradation of PCL-lignin membrane

To investigate the *in vivo* degradation of PCL-lignin50 membrane, macroscopic observation was performed after 10 days of implantation in the joint. And lignin concentration in synovial fluid after 10 days was determined by a lignin assay kits (Solarbio, China) according to the instructions provided by the manufacturer. As comparison, intra-articular injection of lignin (1.0 mL,100 mg/mL) was also performed.

ELISA measurement of *MMP-13* and *IL-6 in vivo*

Quantification of *MMP-13* and *IL-6* in the joint fluid was performed by an ELISA with an ELISA kit (R&D Systems, USA) according to the instructions provided by the

manufacturer. The plates were read at 450 nm wavelength using a plate reader (Thermo Fisher, USA).

Macroscopic observation and histological examination

Macroscopic observation was conducted by two independent observers blinded to the experiments. The lesions in the articular cartilage were graded based on a 0–4 scale described by Pelletier et al.[67], where a higher score indicates greater cartilage damage.

The histological evaluation was performed by HE staining, toluidine blue, safranin O-fast green, and Alcian blue staining. Briefly, after fixing with 4% (v/v) paraformaldehyde for 48 h and decalcification with ethylenediaminetetraacetic acid decalcifying fluid (Boster, China), the cartilage tissues were embedded in paraffin and cut into serial sections of 3 μm. The sections were dewaxed and detected by using HE, Toluidine Blue Cartilage, Modified Safranine O-Fast Green FCF Cartilage, and Alcian Blue Cartilage staining kits (Solarbio, China) according to the instructions provided by the manufacturer. Images were acquired using a microscope (Olympus, Japan). The severity of the OA lesions in the medial tibial plateaus was graded using OARSI scoring system, which is the gold standard for cartilage damage evaluation[67]. The scoring was based on the most severe histologic changes within each cartilage section[68].

Statistical analysis

All data is expressed as means ± SD or as the median (scatter grams), and statistical analysis was carried out using one-way analysis of variance (ANOVA) followed by Least Significant Difference (LSD) test if the results were significant or Mann-Whitney

U test (macroscopic score). *P* values less than 0.05 were considered statistically significant. All experiments were performed in triplicate or duplicate.

Acknowledgments

This study was financially supported by National key research and development program of China (2018YFC1105900), the Guangxi Scientific Research and Technological Development Foundation (Grant No. GuikeAB16450003)，and the local Science and Technology Development Project leading by the central government (the three-D printing and digital medical platform, Grant No. GuikeZY18164004), High level innovation teams and outstanding scholars in Guangxi Universities (The third batch). The authors gratefully acknowledge the financial support from the Institute of Materials Research and Engineering (IMRE) under the Agency of Science, Technology and Research (A*STAR).

Conflict of Interest

The authors declare no conflict of interest

Data availability

All of the data reported in this work are available upon request.

Reference

[1] O. Altindag, O. Erel, N. Aksoy, S. Selek, H. Celik, M. Karaoglanoglu, Increased oxidative stress and its relation with collagen metabolism in knee osteoarthritis, Rheumatology international 27(4) (2007) 339-44.
[2] J. Sherwood, Osteoarthritis year in review 2018: biology, Osteoarthritis and cartilage 27(3) (2019) 365-370.
[3] M. Varela-Eirin, J. Loureiro, E. Fonseca, S. Corrochano, J.R. Caeiro, M. Collado, M.D. Mayan, Cartilage regeneration and ageing: Targeting cellular plasticity in osteoarthritis, Ageing research reviews 42 (2018) 56-71.
[4] M. Rahmati, G. Nalesso, A. Mobasheri, M. Mozafari, Aging and osteoarthritis: Central role of the extracellular matrix, Ageing research reviews 40 (2017) 20-30.
[5] J.A. Bolduc, J.A. Collins, R.F. Loeser, Reactive oxygen species, aging and articular cartilage homeostasis, Free radical biology & medicine 132 (2019) 73-82.
[6] K. Yudoh, T. Nguyen v, H. Nakamura, K. Hongo-Masuko, T. Kato, K. Nishioka, Potential involvement of oxidative stress in cartilage senescence and development of osteoarthritis: oxidative stress induces chondrocyte telomere instability and downregulation of chondrocyte function, Arthritis research & therapy 7(2) (2005) R380-91.
[7] J.S. Gibson, P.I. Milner, R. White, T.P. Fairfax, R.J. Wilkins, Oxygen and reactive oxygen species in articular cartilage: modulators of ionic homeostasis, Pflugers Archiv : European journal of physiology 455(4) (2008) 563-73.
[8] K. Morita, T. Miyamoto, N. Fujita, Y. Kubota, K. Ito, K. Takubo, K. Miyamoto, K. Ninomiya, T. Suzuki, R. Iwasaki, M. Yagi, H. Takaishi, Y. Toyama, T. Suda, Reactive oxygen species induce chondrocyte hypertrophy in endochondral ossification, The Journal of experimental medicine 204(7) (2007) 1613-23.
[9] S. Portal-Nunez, P. Esbrit, M.J. Alcaraz, R. Largo, Oxidative stress, autophagy, epigenetic changes and regulation by miRNAs as potential therapeutic targets in osteoarthritis, Biochemical pharmacology 108 (2016) 1-10.
[10] P. Lepetsos, A.G. Papavassiliou, ROS/oxidative stress signaling in osteoarthritis, Biochimica et biophysica acta 1862(4) (2016) 576-591.
[11] L.J. Ignarro, J.M. Fukuto, J.M. Griscavage, N.E. Rogers, R.E. Byrns, Oxidation of nitric oxide in aqueous solution to nitrite but not nitrate: comparison with enzymatically formed nitric oxide from L-arginine, Proceedings of the National Academy of Sciences of the United States of America 90(17) (1993) 8103-7.
[12] R.F. Loeser, C.S. Carlson, M. Del Carlo, A. Cole, Detection of nitrotyrosine in aging and osteoarthritic cartilage: Correlation of oxidative damage with the presence of interleukin-1beta and with chondrocyte resistance to insulin-like growth factor 1, Arthritis and rheumatism 46(9) (2002) 2349-57.
[13] A.K. Grover, S.E. Samson, Benefits of antioxidant supplements for knee osteoarthritis: rationale and reality, Nutrition journal 15 (2016) 1.
[14] K.Y. Chin, S. Ima-Nirwana, The Role of Vitamin E in Preventing and Treating Osteoarthritis - A Review of the Current Evidence, Frontiers in pharmacology 9 (2018) 946.
[15] Q. Chen, X. Shao, P. Ling, F. Liu, G. Han, F. Wang, Recent advances in polysaccharides for osteoarthritis therapy, European journal of medicinal chemistry 139 (2017) 926-935.

[16] G. Zhong, X. Yang, X. Jiang, A. Kumar, H. Long, J. Xie, L. Zheng, J. Zhao, Dopamine-melanin nanoparticles scavenge reactive oxygen and nitrogen species and activate autophagy for osteoarthritis therapy, Nanoscale 11(24) (2019) 11605-11616.
[17] Y. Pei, F. Cui, X. Du, G. Shang, W. Xiao, X. Yang, Q. Cui, Antioxidative nanofullerol inhibits macrophage activation and development of osteoarthritis in rats, International journal of nanomedicine 14 (2019) 4145-4155.
[18] Y.S. Li, F.J. Zhang, C. Zeng, W. Luo, W.F. Xiao, S.G. Gao, G.H. Lei, Autophagy in osteoarthritis, Joint, bone, spine : revue du rhumatisme 83(2) (2016) 143-8.
[19] A.S. Marchev, P.A. Dimitrova, A.J. Burns, R.V. Kostov, A.T. Dinkova-Kostova, M.I. Georgiev, Oxidative stress and chronic inflammation in osteoarthritis: can NRF2 counteract these partners in crime?, Annals of the New York Academy of Sciences 1401(1) (2017) 114-135.
[20] N.M. Khan, I. Ahmad, T.M. Haqqi, Nrf2/ARE pathway attenuates oxidative and apoptotic response in human osteoarthritis chondrocytes by activating ERK1/2/ELK1-P70S6K-P90RSK signaling axis, Free radical biology & medicine 116 (2018) 159-171.
[21] V.K. Ponnusamy, D.D. Nguyen, J. Dharmaraja, S. Shobana, J.R. Banu, R.G. Saratale, S.W. Chang, G. Kumar, A review on lignin structure, pretreatments, fermentation reactions and biorefinery potential, Bioresource technology 271 (2019) 462-472.
[22] M. Witzler, A. Alzagameem, M. Bergs, B.E. Khaldi-Hansen, S.E. Klein, D. Hielscher, B. Kamm, J. Kreyenschmidt, E. Tobiasch, M. Schulze, Lignin-Derived Biomaterials for Drug Release and Tissue Engineering, 23(8) (2018).
[23] W. Schutyser, T. Renders, S. Van den Bosch, S.F. Koelewijn, G.T. Beckham, B.F. Sels, Chemicals from lignin: an interplay of lignocellulose fractionation, depolymerisation, and upgrading, Chemical Society reviews 47(3) (2018) 852-908.
[24] A. Majira, B. Godon, L. Foulon, J. van der Putten, L. Cezard, M. Thierry, F. Pion, A. Bado-Nilles, P. Pandard, T. Jayabalan, V. Aguie-Beghin, P.H. Ducrot, C. Lapierre, G. Marlair, R.J.A. Gosselink, S. Baumberger, B. Cottyn, Enhancing the antioxidant activity of technical lignins by combining solvent fractionation and ionic liquid treatment, ChemSusChem (2019).
[25] C. Wang, S.S. Kelley, R.A. Venditti, Lignin-Based Thermoplastic Materials, ChemSusChem 9(8) (2016) 770-83.
[26] X. Liu, E. Zong, J. Jiang, S. Fu, J. Wang, B. Xu, W. Li, X. Lin, Y. Xu, C. Wang, F. Chu, Preparation and characterization of Lignin-graft-poly (varepsilon-caprolactone) copolymers based on lignocellulosic butanol residue, International journal of biological macromolecules 81 (2015) 521-9.
[27] Y. Pang, L. Xin, S. Wang, X. Qiu, D. Yang, H. Lou, Lignin-polyurea microcapsules with anti-photolysis and sustained-release performances synthesized via pickering emulsion template, Reactive & Functional Polymers 123 (2018) 115-121.
[28] M.A. Salami, F. Kaveian, M. Rafienia, S. Saber-Samandari, A. Khandan, M. Naeimi, Electrospun Polycaprolactone/lignin-based Nanocomposite as a Novel Tissue Scaffold for Biomedical Applications, Journal of medical signals and sensors 7(4) (2017) 228-238.
[29] J. Wang, L. Tian, B. Luo, S. Ramakrishna, D. Kai, X.J. Loh, I.H. Yang, G.R. Deen, X. Mo, Engineering PCL/lignin nanofibers as an antioxidant scaffold for the growth of neuron and Schwann cell, Colloids and surfaces. B, Biointerfaces 169 (2018) 356-365.

[30] D. Lin, L. Rui, L. Hu, Z. Zou, C. Si, Lignin nanoparticle as a novel green carrier for the efficient delivery of resveratrol, Acs Sustainable Chemistry & Engineering 5(9) (2017) acssuschemeng.7b01903.
[31] V.K. Thakur, M.K. Thakur, Recent advances in green hydrogels from lignin: a review, International journal of biological macromolecules 72 (2015) 834-47.
[32] M.H. Sipponen, H. Lange, C. Crestini, A. Henn, M. Osterberg, Lignin for Nano- and Microscaled Carrier Systems: Applications, Trends, and Challenges, ChemSusChem 12(10) (2019) 2039-2054.
[33] M. Witzler, A. Alzagameem, M. Bergs, B.E. Khaldi-Hansen, S.E. Klein, D. Hielscher, B. Kamm, J. Kreyenschmidt, E. Tobiasch, M. Schulze, Lignin-Derived Biomaterials for Drug Release and Tissue Engineering, Molecules (Basel, Switzerland) 23(8) (2018).
[34] K. Dan, K. Zhang, J. Lu, Z.W. Hua, Z. Li, Z. Zheng, J.L. Xian, Sustainable and antioxidant lignin-polyester copolymers and nanofibers for potential healthcare applications, Acs Sustainable Chemistry & Engineering 5(7) (2017) acssuschemeng.7b00850.
[35] A.R. Armiento, M.J. Stoddart, M. Alini, D. Eglin, Biomaterials for articular cartilage tissue engineering: Learning from biology, Acta biomaterialia 65 (2018) 1-20.
[36] J. Xue, J. Xie, W. Liu, Y. Xia, Electrospun Nanofibers: New Concepts, Materials, and Applications, Accounts of chemical research 50(8) (2017) 1976-1987.
[37] H. Liu, H. Chung, Self-Healing Properties of Lignin-Containing Nanocomposite: Synthesis of Lignin-graft-poly(5-acetylaminopentyl acrylate) via RAFT and Click Chemistry, Macromolecules 49(19) (2016) 7246-7256.
[38] W. Ren, X. Pan, G. Wang, W. Cheng, Y. Liu, Dodecylated lignin-g-PLA for effective toughening of PLA, Green Chemistry (18) (2016) 5008-5014
[39] D. Kai, K. Zhang, L. Jiang, H.Z. Wong, Z. Li, Z. Zhang, X.J. Loh, Sustainable and Antioxidant Lignin–Polyester Copolymers and Nanofibers for Potential Healthcare Applications, ACS Sustainable Chemistry & Engineering 5(7) (2017) 6016-6025.
[40] J. Alamed, W. Chaiyasit, D.J. McClements, E.A. Decker, Relationships between free radical scavenging and antioxidant activity in foods, Journal of agricultural and food chemistry 57(7) (2009) 2969-76.
[41] Z. Can, O. Yildiz, H. Sahin, E. Akyuz Turumtay, S. Silici, S. Kolayli, An investigation of Turkish honeys: their physico-chemical properties, antioxidant capacities and phenolic profiles, Food chemistry 180 (2015) 133-141.
[42] U. Adhikari, X. An, N. Rijal, T. Hopkins, S. Khanal, T. Chavez, R. Tatu, J. Sankar, K.J. Little, D.B. Hom, N. Bhattarai, S.K. Pixley, Embedding magnesium metallic particles in polycaprolactone nanofiber mesh improves applicability for biomedical applications, Acta biomaterialia (2019).
[43] K. Ren, Y. Wang, T. Sun, W. Yue, H. Zhang, Electrospun PCL/gelatin composite nanofiber structures for effective guided bone regeneration membranes, Materials science & engineering. C, Materials for biological applications 78 (2017) 324-332.
[44] W. Hu, K. Murata, D. Zhang, Applicability of LIVE/DEAD BacLight stain with glutaraldehyde fixation for the measurement of bacterial abundance and viability in rainwater, Journal of environmental sciences (China) 51 (2017) 202-213.
[45] H. Li, D. Wang, Y. Yuan, J. Min, New insights on the MMP-13 regulatory network in the pathogenesis of early osteoarthritis, Arthritis research & therapy 19(1) (2017) 248.

[46] D. Dutta, J. Xu, J.S. Kim, W.A. Dunn, Jr., C. Leeuwenburgh, Upregulated autophagy protects cardiomyocytes from oxidative stress-induced toxicity, Autophagy 9(3) (2013) 328-44.
[47] Y. Ichimura, S. Waguri, Y.S. Sou, S. Kageyama, J. Hasegawa, R. Ishimura, T. Saito, Y. Yang, T. Kouno, T. Fukutomi, T. Hoshii, A. Hirao, K. Takagi, T. Mizushima, H. Motohashi, M.S. Lee, T. Yoshimori, K. Tanaka, M. Yamamoto, M. Komatsu, Phosphorylation of p62 activates the Keap1-Nrf2 pathway during selective autophagy, Molecular cell 51(5) (2013) 618-31.
[48] M. Komatsu, H. Kurokawa, S. Waguri, K. Taguchi, A. Kobayashi, Y. Ichimura, Y.S. Sou, I. Ueno, A. Sakamoto, K.I. Tong, M. Kim, Y. Nishito, S. Iemura, T. Natsume, T. Ueno, E. Kominami, H. Motohashi, K. Tanaka, M. Yamamoto, The selective autophagy substrate p62 activates the stress responsive transcription factor Nrf2 through inactivation of Keap1, Nature cell biology 12(3) (2010) 213-23.
[49] W. Tu, H. Wang, S. Li, Q. Liu, H. Sha, The Anti-Inflammatory and Anti-Oxidant Mechanisms of the Keap1/Nrf2/ARE Signaling Pathway in Chronic Diseases, Aging and disease 10(3) (2019) 637-651.
[50] J.A. Collins, B.O. Diekman, R.F. Loeser, Targeting aging for disease modification in osteoarthritis, Current opinion in rheumatology 30(1) (2018) 101-107.
[51] C. Vinatier, C. Merceron, J. Guicheux, Osteoarthritis: from pathogenic mechanisms and recent clinical developments to novel prospective therapeutic options, Drug discovery today 21(12) (2016) 1932-1937.
[52] W. Zhang, W.B. Robertson, J. Zhao, W. Chen, J. Xu, Emerging Trend in the Pharmacotherapy of Osteoarthritis, Frontiers in endocrinology 10 (2019) 431.
[53] W. Hermann, S. Lambova, U. Muller-Ladner, Current Treatment Options for Osteoarthritis, Current rheumatology reviews 14(2) (2018) 108-116.
[54] R.R. Bannuru, M.C. Osani, E.E. Vaysbrot, N.K. Arden, K. Bennell, S.M.A. Bierma-Zeinstra, V.B. Kraus, L.S. Lohmander, J.H. Abbott, M. Bhandari, F.J. Blanco, R. Espinosa, I.K. Haugen, J. Lin, L.A. Mandl, E. Moilanen, N. Nakamura, L. Snyder-Mackler, T. Trojian, M. Underwood, T.E. McAlindon, OARSI guidelines for the non-surgical management of knee, hip, and polyarticular osteoarthritis, Osteoarthritis and cartilage (2019).
[55] S. Gopalakrishnan, S. Thomas, N. Kalazikkal, OSC21: Morphological, Mechanical and Biological Properties of Silver Nanoparticle Decorated Denture Base Polymer, Journal of Indian Prosthodontic Society 18(Suppl 1) (2018) S16.
[56] S. Mohan, O.S. Oluwafemi, S.C. George, V.P. Jayachandran, F.B. Lewu, S.P. Songca, N. Kalarikkal, S. Thomas, Completely green synthesis of dextrose reduced silver nanoparticles, its antimicrobial and sensing properties, Carbohydrate polymers 106 (2014) 469-74.
[57] K.S. Joshy, A. George, J. Jose, N. Kalarikkal, L.A. Pothen, S. Thomas, Novel dendritic structure of alginate hybrid nanoparticles for effective anti-viral drug delivery, International journal of biological macromolecules 103 (2017) 1265-1275.
[58] R. Augustine, F. Sarry, N. Kalarikkal, S. Thomas, L. Badie, D. Rouxel, Surface Acoustic Wave Device with Reduced Insertion Loss by Electrospinning P(VDF-TrFE)/ZnO Nanocomposites, Nano-micro letters 8(3) (2016) 282-290.
[59] K. Ghosal, B.T. Hazra, B.B. Bhowmik, S. Thomas, Formulation Development, Physicochemical Characterization and In Vitro-In Vivo Drug Release of Vaginal Films, Current HIV research 14(4) (2016) 295-306.

[60] I. Raj, M. Mozetic, V.P. Jayachandran, J. Jose, S. Thomas, N. Kalarikkal, Fracture resistant, antibiofilm adherent, self-assembled PMMA/ZnO nanoformulations for biomedical applications: physico-chemical and biological perspectives of nano reinforcement, Nanotechnology 29(30) (2018) 305704.
[61] K. Chen, X. Lv, Autophagy Is a Protective Response to the Oxidative Damage to Endplate Chondrocytes in Intervertebral Disc: Implications for the Treatment of Degenerative Lumbar Disc, 2017 (2017) 4041768.
[62] N. Hariharan, P. Zhai, J. Sadoshima, Oxidative stress stimulates autophagic flux during ischemia/reperfusion, Antioxidants & redox signaling 14(11) (2011) 2179-90.
[63] K. Lampropoulou-Adamidou, P. Lelovas, E.V. Karadimas, C. Liakou, I.K. Triantafillopoulos, I. Dontas, N.A. Papaioannou, Useful animal models for the research of osteoarthritis, European journal of orthopaedic surgery & traumatology : orthopedie traumatologie 24(3) (2014) 263-71.
[64] P.X. Ling, L.N. Zhang, Y. Jin, Y.L. He, T.M. Zhang, Effects of a hyaluronic acid and low molecular weight heparin injection on osteoarthritis in rabbits, Drug discoveries & therapeutics 3(4) (2009) 146-50.
[65] A.M. McCoy, Animal Models of Osteoarthritis: Comparisons and Key Considerations, Veterinary pathology 52(5) (2015) 803-18.
[66] S. Cetrullo, S. D'Adamo, S. Guidotti, R.M. Borzi, F. Flamigni, Hydroxytyrosol prevents chondrocyte death under oxidative stress by inducing autophagy through sirtuin 1-dependent and -independent mechanisms, Biochimica et biophysica acta 1860(6) (2016) 1181-91.
[67] K.P. Pritzker, S. Gay, S.A. Jimenez, K. Ostergaard, J.P. Pelletier, P.A. Revell, D. Salter, W.B. van den Berg, Osteoarthritis cartilage histopathology: grading and staging, Osteoarthritis and cartilage 14(1) (2006) 13-29.
[68] R.W. Moskowitz, Osteoarthritis cartilage histopathology: grading and staging, Osteoarthritis and cartilage 14(1) (2006) 1-2.